Published online 4 November 2013 *Nucleic Acids Research, 2014, Vol. 42, No. 3* ***1575–1592***
doi:10.1093/nar/gkt1033

SUMOylation regulates the chromatin occupancy and anti-proliferative gene programs of glucocorticoid receptor

Ville Paakinaho[1], Sanna Kaikkonen[1], Harri Makkonen[1], Vladimir Benes[2] and Jorma J. Palvimo[1,3,*]

[1]Institute of Biomedicine, University of Eastern Finland, Kuopio, PO Box 1627, FI-70211 Kuopio, Finland, [2]European Molecular Biology Laboratory (EMBL), Core Facilities and Services, Meyerhofstrasse 1, 69117 Heidelberg, Germany and [3]Department of Pathology, Kuopio University Hospital, Kuopio, Finland

Received July 18, 2013; Revised September 20, 2013; Accepted October 9, 2013

ABSTRACT

In addition to the glucocorticoids, the glucocorticoid receptor (GR) is regulated by post-translational modifications, including SUMOylation. We have analyzed how SUMOylation influences the activity of endogenous GR target genes and the receptor chromatin binding by using isogenic HEK293 cells expressing wild-type GR (wtGR) or SUMOylation-defective GR (GR3KR). Gene expression profiling revealed that both dexamethasone up- and downregulated genes are affected by the GR SUMOylation and that the affected genes are significantly associated with pathways of cellular proliferation and survival. The GR3KR-expressing cells proliferated more rapidly, and their anti-proliferative response to dexamethasone was less pronounced than in the wtGR-expressing cells. ChIP-seq analyses indicated that the SUMOylation modulates the chromatin occupancy of GR on several loci associated with cellular growth in a fashion that parallels with their differential dexamethasone-regulated expression between the two cell lines. Moreover, chromatin SUMO-2/3 marks, which were associated with active GR-binding sites, showed markedly higher overlap with the wtGR cistrome than with the GR3KR cistrome. In sum, our results indicate that the SUMOylation does not simply repress the GR activity, but regulates the activity of the receptor in a target locus selective fashion, playing an important role in controlling the GR activity on genes influencing cell growth.

INTRODUCTION

Glucocorticoid receptor (GR) is a hormone-controlled transcription factor belonging to the nuclear receptor superfamily (1). The GR is activated by natural and synthetic glucocorticoids that are among the most widely prescribed pharmaceuticals worldwide because of their anti-inflammatory effects (2). On binding of the ligand, the GR moves to nucleus and binds with high affinity to short DNA-sequences, glucocorticoid response elements (GREs) on chromatin where it influences transcription by recruiting various coregulators including chromatin-remodeling complexes (1,3–5). The anti-inflammatory effect of GR has been thought to be largely due to its capability to inhibit the action of activator protein 1 (AP-1) and nuclear factor-κB (NF-κB) by directly interacting with them or indirectly e.g. by inducing the expression of *NFKBIA* gene that encodes the NF-κB inhibitor IκBα (6–8). The GR is also capable of inducing apoptosis (9) and cell cycle arrest (10) of certain cell types by affecting to the expression of genes such as *Bcl-2*, *NFKBIA* and cyclin-dependent protein kinase inhibitors (*CDKN*).

In addition to the glucocorticoids, post-translational modifications, such as phosphorylation and SUMOylation, regulate the activity of GR (11–14). In SUMOylation, small ubiquitin-related modifier proteins (SUMOs) are covalently conjugated to specific lysine residues of target proteins. The major group of SUMO targets resides in the nucleus and it includes several nuclear receptors (15). Humans express three SUMO proteins, SUMO-1, -2 and -3, that can form isopeptide linkages with specific lysine residues of target proteins. SUMO-2 and -3 are practically identical (from herein called SUMO-2/3), but SUMO-1 is only ∼50% identical with SUMO-2/3 (16,17). The SUMOylation pathway is similar to that of ubiquitylation pathway, but the E1, E2 and E3 enzymes are specific for the SUMOylation (18,19).

*To whom correspondence should be addressed. Tel: +358 40 5910693; Fax: +353 17 162889; Email: jorma.palvimo@uef.fi

Activation of SUMOs occurs through SAE1 and -2 dimer (E1) and UBC9 (E2) conjugates SUMOs to target proteins (20). SUMO modifications are highly dynamic and shown to be reversed (deSUMOylated) by a family of SUMO-specific proteases (SENP1, -2, -3, -5, -6 and -7) (21,22). The essential nature of SUMOylation for mammalian development is demonstrated by the *Ubc9* knockout mice that show embryonic lethality (23).

Interestingly, UBC9, protein inhibitor of activated STAT (PIAS) proteins (SUMO E3 ligases) and SENP1 and -2 can function as coregulators for steroid receptors (19,24). SUMO modifications of transcription factors have been often linked to transcriptional repression (15). However, these notions are mainly based on the usage of ectopically expressed transcription factors and reporter genes. The repression has been suggested to be due to association of SUMOylated transcription factors with SUMO-binding corepressors, such as DAXX (death domain-associated protein) (25,26). However, accumulating evidence implies that the SUMOylation does not merely repress transcription factor activity. For example, intact SUMOylation sites of androgen receptor (AR) are needed for the receptor's full transcriptional activity on many target genes (27).

We and others have previously shown that the SUMO conjugation sites in the GR act as synergy control motifs restricting the transcriptional activity of the receptor on a minimal promoter driven by two or more GREs, but not on a more complex natural mouse mammary tumor virus promoter (11,28). There may also be cross-talk between the GR SUMOylation and the receptor phosphorylation by c-Jun N-terminal kinase in the regulation of glucocorticoid signaling (14). Furthermore, the inhibitory effect of SUMOylated GR is not dependent on the SUMO-binding protein DAXX, but on some other factor that is preferentially recruited on promoters with multiple GREs (29). However, there is scarce information about the role of SUMOylation in the regulation of endogenous GR target genes. Here, we have investigated in an unbiased fashion how GR SUMOylation influences the GR activity in a natural chromatin environment by using genome-wide methods. To that end, we used isogenic cell lines stably expressing either wild-type GR (wtGR) or SUMOylation-site mutated GR (GR3KR) using human embryonal kidney (HEK293) cells that contain low (nonfunctional) levels of GR and have been previously found useful for studying GR signaling (30). Our transcriptome and cistrome analyses reveal for the first time that the GR SUMOylation sites regulate the receptor's chromatin occupancy and function in a target locus-selective fashion and that the genes differently expressed by glucocorticoid due to the GR SUMOylation sites are significantly enriched in cell proliferation and apoptosis pathways. In addition, our ChIP-seq data reveal that a significant portion of chromatin-bound SUMO-2/3 overlaps with the GR cistrome in the HEK293 cells.

MATERIALS AND METHODS

Plasmid constructions

For generation of pcDNA5/FRT-hGR, pcDNA5/FRT-hGR3KR, pcDNA3.1-hGR and pcDNA3.1-hGR3KR, complementary DNAs (cDNAs) from pSG5-hGR and pSG5-hGR-K277,293,703R (11) were transferred as BamHI fragments into pcDNA5/FRT or pcDNA3.1(+) (Invitrogen) backbone. The plasmids described were verified by sequencing.

Cell culture

Stably GR expressing isogenic HEK293 (Flp-In^{TM}-293, Invitrogen) cells lines were generated according to manufacturer's instructions and as described (27). Flp-In^{TM}-293 cells grown on 10-cm dishes were cotransfected with 9:1 ratio of pOG44:pcDNA5/FRT-hGR or pcDNA5/FRT-hGR-3KR using Lipofectamine 2000 (Invitrogen). Forty-eight hours after transfection, the cells were divided 1:2 and hygromycin-B (100 μg/ml) (Invitrogen) was added. Thereafter, cells received fresh hygromycin-supplemented medium every 3 days and were grown for 19 days. Twelve hygromycin-resistant foci were picked in each culture with pipette tips and transferred to 24-well plate wells, grown for 8 days and transferred to 12 wells for further growth and analyses. These wells were divided to four portions for Zeocin^{TM} (Invitrogen) sensitivity test, β-galactosidase assay, GR expression analyses and further growth. Three equivalent clones of both GR forms were further analyzed for expression of endogenous GR target genes, and one representative clone was chosen for further experiments. The stably GR-expressing HEK293 cell lines were maintained in Dulbecco's modified Eagle's medium (Gibco®, Invitrogen) supplemented with 10% (v/v) fetal bovine serum, 25 U/ml penicillin and 25 μg/ml streptomycin and 100 μg/ml hygromycin-B. U2 osteosarcoma (U2Os) cells [American Type Culture Collection (ATCC)] were transfected with 15 μg of pcDNA3.1-hGR or pcDNA3.1-hGR-K277,293,703R using TransIT-LT1 (Mirus Bio Corporation) transfection reagent. Forty-eight hours after transfection, the cells were split to 1:2 and geneticin (400 μg/ml) was added. Medium containing geneticin was replaced every third day. Two weeks after transfection, the cells were split to RNA and western blot analyses and further growth. Based on these analyses, one representative clone for both GR forms was picked for further experiments. The stably GR-expressing U2Os cell lines were maintained in Dulbecco's modified Eagle's medium supplemented with 10% fetal bovine serum, 1 mM Na-puryvate, 25 U/ml penicillin and 25 μg/ml streptomycin and 400 μg/ml geneticin.

Antibodies

Anti-GR (sc-1003) and normal rabbit IgG (sc-2027) were from Santa Cruz Biotechnology, anti-SUMO-1 (33–2400) was from Invitrogen Life Technologies and anti-SUMO-2/3 (M114-3) was from MBL International Corporation.

Cell proliferation assay

For proliferation assays, both empty HEK293 (Flp-In^{TM}-293 cells, background), wtGR- and GR3KR-expressing HEK293 cells were seeded onto 96-well plates (5000 cells/well). Cells were grown for 48 h before addition of 100 nM dexamethasone (dex). At indicated time points, six parallel samples of the cells were analyzed by using Cell Titer96 Aqueous cell proliferation assay reagent

(Promega) according to manufacturer's instructions. The quantity of formazan reaction product as measured by the absorbance at 492 nm is directly proportional to the number of metabolically active living cells in culture.

Fluorescence-activated cell sorting

For cell cycle analysis, HEK293 cells were seeded on 12-well plates and grown ± dex and after 48 h, cells were trypsinized, suspensed into phosphate-buffered saline (PBS) and fixed in ice cold 70% ethanol. After overnight incubation at 4°C, cells were centrifuged, resuspensed into PBS containing 150 μg/ml RNase A (Fermentas) and incubated for 1 h at 50°C. To stain DNA, 8 μg/ml final concentration of propidium jodide was added to the samples and incubated for 2 h at 37°C in dark. Measurements of DNA contents of triplicate samples were performed with fluorescence-activated cell sorting (FACS) Canto II flow cytometer using BD FACS Diva Flow Cytometer Software (Becton Dickinson).

Isolation of RNA and RT-qPCR analyses

Stably GR-expressing HEK293 and U2Os cells were seeded onto 6-well plates (300 000 and 250 000 cells/well, respectively) and grown 36 h in steroid-depleted transfection medium. Subsequently, cells were treated either with vehicle (ethanol, 0.01%) or 100 nM of dex for 6 h. Total RNA was extracted using TriPure (Roche) and converted to cDNA using Transcriptor First Strand cDNA synthesis Kit (Roche Diagnostics GmbH, Mannheim, Germany) according to manufacturer's instructions. cDNA was used as a template in RT-qPCR, which was carried out using LightCycler® 480 SYBR Green I Master (Roche Diagnostics GmbH) and LightCycler® 480 System (Roche) and with specific primers listed in Supplementary Table S1. Analyzed RPL13A messenger RNA levels were used to normalize the amounts of total RNA between the samples. Fold changes were calculated using the formula $2^{-(\Delta\Delta Ct)}$, where $\Delta\Delta Ct$ is $\Delta Ct_{(dex)}-\Delta Ct_{(EtOH)}$, ΔCt is $Ct_{(gene\ X)}-Ct_{(RPL13A)}$ and Ct is the cycle at which the threshold is crossed.

Microarray analysis

Total RNA was analyzed on Sentrix HumanHT-12 v4 Expression BeadChips (Illumina) using the manufacturer's protocol at the Finnish Microarray and Sequencing Center (Turku, Finland). Microarray data were analyzed within R software version 2.13.0. (http://www.r-project.org/) using the Bioconductor package lumi [(31), http://www.bioconductor.org/] and normalized using VST transformation and RSN normalization used as standard approach for Illumina arrays. Differentially expressed genes were analyzed with limma package, with linear model fitting for statistical analyses by empirical Bayes method. The *P*-values were adjusted with the Benjamini and Hochberg method to control the false discovery rate (FDR). Biological comparisons were made, for example dex/vehicle GR3KR or dex/vehicle wtGR and dex/vehicle GR3KR versus dex/vehicle wtGR. Heat maps were generated by using heatmap.2 in the R package gplots. Unsupervised hierarchical clustering of genes was performed using Euclidean distance and complete linkage. Ingenuity Pathway Analysis® (IPA) was used to identify biological processes differently enriched between wtGR- and GR3KR-expressing cells.

ChIP and DNA deep sequencing

Stably GR-expressing cells were seeded at ~70% confluence onto 175 cm^2 bottles and allowed to grow in steroid-depleted transfection medium for 72 h prior ChIP. Cells were treated either with vehicle or 100 nM of dex for 1 h. The cells were cross-linked by adding formaldehyde to the medium to a final concentration of 1% (v/v) for 10 min at 22°C. The cells were rinsed twice with PBS and collected in a cold room in Farham Lysis Buffer [5 mM PIPES (pH 8.0), 85 mM KCl, 0.5% (v/v) NP-40] containing Roche Complete Protease Inhibitor Cocktail. After centrifugation, the cell pellets were resuspended in RIPA buffer [1× PBS, 1% (v/v) NP-40, 0.5% (w/v) sodium deoxycholate, 0.1% (w/v) sodium dodecyl sulfate, protease inhibitor cocktail]. Chromatin was sonicated to an average DNA length of 200–500 bp and cellular debris was removed by centrifugation. Aliquots of 100 μl of the lysate were diluted 1:10 in RIPA buffer and subjected to immunoprecipitation with 1 μg of indicated antibody coupled onto protein A magnetic beads (Millipore, Temecula, CA, USA) with rotation overnight at 4°C. The beads were harvested by magnets and washed five times for 3 min in cold room by rotation with 1 ml of LiCl IP wash buffer [100 mM Tris (pH 7.5), 500 mM LiCl, 1% (w/v) NP-40, 1% (w/v) sodium deoxycholate]. Finally, the beads were washed two times with 1 ml of TE buffer [1 mM EDTA, 10 mM Tris-HCl (pH 8.1)], and antibody-bound chromatin fragments were eluted from the beads by incubation at 65°C for 1 h with elution buffer [1% (w/v) sodium dodecyl sulfate in 0.1 M $NaHCO_3$]. The cross-linking was reversed and the remaining proteins were digested by addition of 40 μg (1.8 U) of proteinase K (Fermentas) and incubation overnight at 65°C. DNA was purified using QIAquick™ PCR purification system (QIAGEN GmbH). ChIP templates were sequenced using Illumina HiSeq System (Illumina) using standard manufacturer protocol at the EMBL Genomics Core Facility (Heidelberg, Germany). For conventional ChIP, quantitative PCR analyses were carried out with LightCycler® 480 SYBR Green I Master (Roche Diagnostics GmbH). Specific primers are listed in Supplementary Table S2. Results were calculated using the formula $E^{-(\Delta Ct)} \times 10$, where E (efficiency of target amplification) is a coefficient of DNA amplification by one PCR cycle for a particular primer pair and ΔCt is $Ct_{(ChIP-template)}-Ct_{(Input)}$. Results are presented as fold over the value IgG-precipitated samples. Re-ChIP analyses (in which chromatin was sequentially precipitated with two different antibodies) were performed essentially as previously (27).

The quality of raw ChIP-seq data was analyzed by FastQC [(32), http://www.bioinformatics.babraham.ac.uk/projects/fastqc/]. Subsequently FASTX-Toolkit [(33), http://hannonlab.cshl.edu/fastx_toolkit/index.html] was used to trim the sequence reads from each ChIP-seq

experiment to 40 bp, and each set was collapsed. The reads were aligned against the human reference genome version hg19 by using Bowtie software version 0.12.9. (34) with the following command line: -e 70 –l 50 –n 1 –k 1 –m 1\–t –p 12 –q –S –best. The generated SAM-file were converted to sorted BAM format by SAM tools (35) and subsequently to TDF format for visualization of the data in Integrative Genomics Viewer (IGV) genome browser (36). The enriched peaks were detected by using MACS program version 1.4.2. (37,38), with the following parameters: for GR samples, bandwidth 100, mfold as 10,30 and 1.0×10^{-4} as *P*-value cutoff; for SUMO-2/3 samples, bandwidth 200, mfold as 10,15 and 1.0×10^{-4} as *P*-value cutoff. MACS estimated FDR value by comparing ChIP-seq data sets with control data set and *vice versa*. Subsequently, the peak detection was performed again to estimate the statistical significance of the peaks. Sequenced input from Flp-FRT cell line was used as control file for GR samples, and sequenced control IgG from Flp-FRT cell line was used as control file for SUMO-2/3 samples. Peaks that were selected for further downstream analysis had the following criteria: tags >50, fold enrichment >8, FDR <0.1 and peak had to be present in two biological replicate samples. The GR peaks selected with these criteria had FDR <0.01 in at least one replicate. Additionally, the same peaks were also found with findPeaks command in HOMER software (http://biowhat.ucsd.edu/homer/). Furthermore, the sequenced samples met the ENDOCE ChIP-seq guidelines, e.g. samples had >10 million uniquely mapped reads, the sequence depth of the controls was at the level equal to ChIP samples. Additionally, all the selected peaks had >75% similarity between replicates or >80% of the top 40% of the selected peaks in one biological replicate were also found in the second biological replicate (39,40). When identifying overlapping peaks, enrichment on chromosome and annotation (CEAS, version 1.0.0.) analysis and motif analysis (SeqPos, version 1.0.0.; Screen motif, version 1.0.0.; MISP, version 1.0.0.) were performed by Cistrome (41). Sequence logos where generated by using the R package seqLogo. Association of genes and peaks (GR or SUMO-2/3-enriched binding sites; GRBs or SUMOBs) was done by using GREAT (42). Kruskal–Wallis one-way analysis of variance was used for comparing the statistical difference in the number of GRBs or that of SUMOBs associated with the dex-regulated genes between the wtGR and the GR3KR cells.

RESULTS

Gene programs regulating cell growth are affected by GR SUMOylation

To study how GR SUMOylation influences gene expression in a genuine chromatin context, we established isogenic HEK293 cell lines stably expressing wtGR or SUMOylation-deficient GR (GR3KR). In the GR3KR, the lysines of the three GR SUMO consensus sites were mutated to arginines, resulting in SUMOylation-deficient GR (11). Immunoblotting indicated that the HEK293 wtGR and GR3KR cells express comparable levels of the receptor and that the level of endogenous GR in the HEK293 background cells is low, lower than that in A549 lung carcinoma cells (Supplementary Figure S1A). Compared with the A549 cells, our HEK293 stable cell lines overexpress the GR. Furthermore, immunoblotting of anti-GR-antibody immunoprecipitates with anti-SUMO-1 or anti-SUMO-2/3 antibody confirmed that the wtGR can become modified by endogenous SUMO-2/3, whereas the GR3KR is severely defective, albeit not totally inert, in this respect (Supplementary Figure S1B) (11). Next, we compared the gene expression profiles of the wtGR and GR3KR cells that were exposed to dex or vehicle for 6 h by using Illumina HT-12 v4 Expression BeadChips. The analysis indicated that more genes were dex-regulated in the GR3KR cells (675) than in the wtGR cells (451), with 59 and 55% of these genes being upregulated by dex in the wtGR and the GR3KR cells, respectively (Figure 1A). All the dex-regulated genes in both cell lines were grouped by unsupervised hierarchical clustering that resulted in eight distinct clusters (clusters 1–8) (Figure 1B). Genes that were up- or downregulated by dex only in wtGR cells were clustered to the cluster 2 and the cluster 5, respectively. The clusters 3 and 7 contained genes up- or downregulated by dex only in GR3KR cells, respectively. The cluster 4 contained genes that were dex-regulated in both cell lines, but had a significant difference in their expression between the wtGR and the GR3KR cells. Genes in the clusters 1, the 6 and 8 were dex-regulated in both cell lines and their gene expression did not markedly differ between the cell lines. Most of the genes that were differently dex-regulated between wtGR and GR3KR cells showed both higher overall dex-induced expression level and fold-induction by dex in one cell line compared with the other (Supplementary Figure S2A). Expression of one gene from each cluster was validated by RT-qPCR analysis (Supplementary Figure S2B). The 483 genes that were differently expressed between the two cell lines (the clusters 2, 3, 4, 5 and 7) were subjected to IPA to find enriched pathways regulated differently due to GR SUMOylation sites. The top six molecular and cellular functions significantly affected by the GR SUMOylation sites were gene expression, cellular development, growth and proliferation, cell death and survival, cellular movement and cell cycle (Figure 1C). We confirmed by RT-qPCR analyses differences in the expression of select dex-upregulated genes that are well-known GR targets associated with the above cellular growth pathways. As shown in Figure 1D, *CDKN1C* (43) and *NFKBIA* (7) were dex-regulated in both cell lines, but they had a significantly higher dex-induced expression levels in the wtGR than the GR3KR cells. Conversely, the dex-induced expression level of *ELK1* and that of *RASD1* were significantly higher in the GR3KR cells. *MAFB* showed dex-upregulation only the wtGR cells and *MERTK* only the GR3KR cells. Interestingly, these GR target genes that showed higher expression levels in the wtGR cells have anti-proliferative effects, whereas those that displayed elevated expressions in the GR3KR cells promote cell proliferation. These results imply that

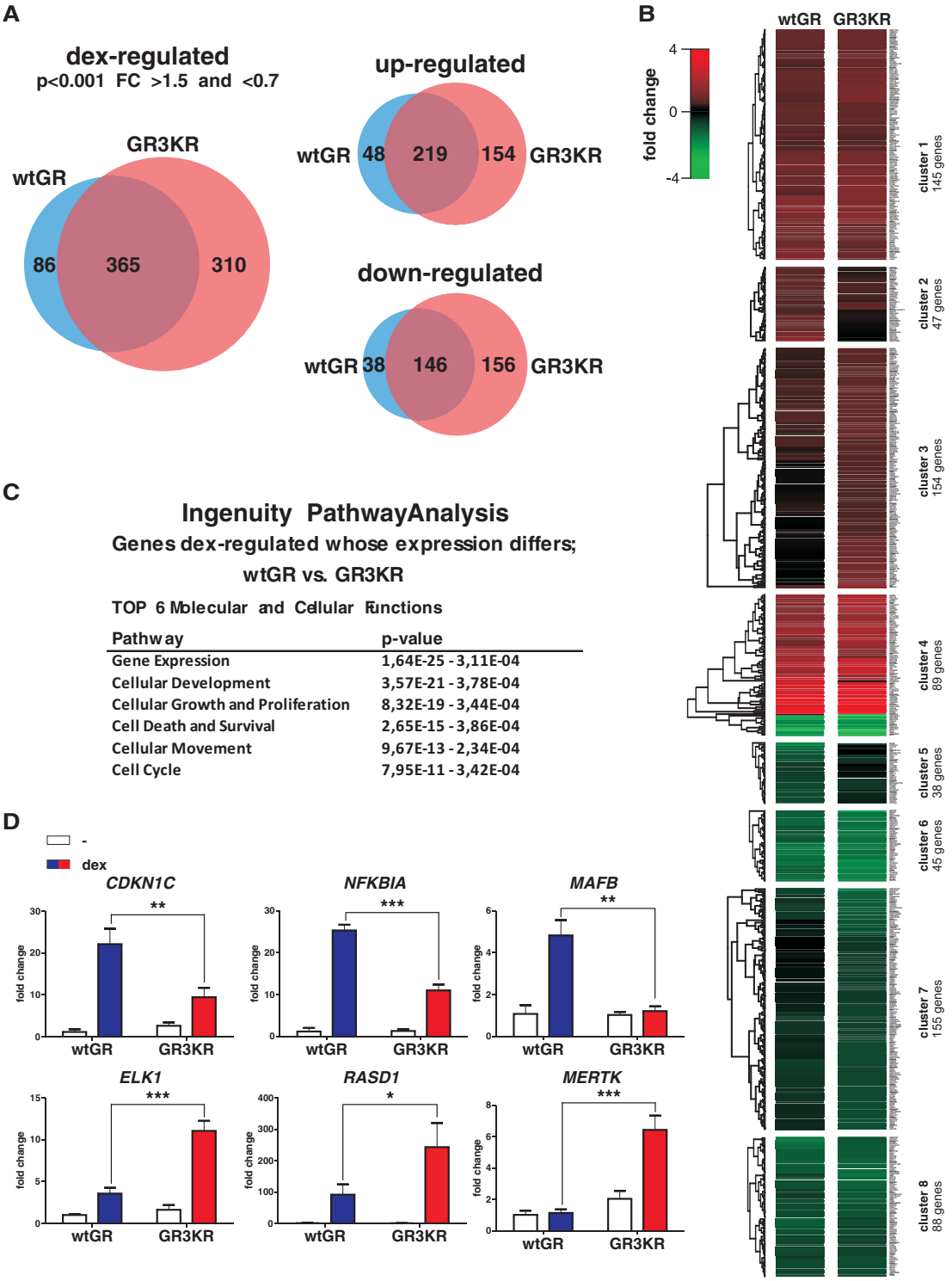

Figure 1. Glucocorticoid target genes affecting cell growth are differently expressed between wtGR- and GR3KR-expressing HEK293 cells. Cell lines were treated with vehicle or dex for 6 h, RNA was isolated and analyzed by Illumina BeadChips as described in 'Materials and Methods' section. The genes that had $P < 0.001$ and fold-induction > 1.5 or < 0.7 were considered as dex-regulated genes: 761 genes of 15 784 genes in the array were dex-regulated. (**A**) Venn diagrams showing comparison of all the genes dex-regulated between the wtGR- (blue) and the GR3KR-expressing cells (red), and additionally dex-up- and downregulated genes in separate diagrams. Values inside the diagram indicate the number of dex-regulated genes shared and unique to each cell line. (**B**) The dex-regulated genes were clustered by unsupervised hierarchical clustering, which resulted in eight clusters of genes shown as heat map: clusters 2 and 5 genes dex-regulated only in wtGR cells, clusters 3 and 7 genes dex-regulated only in GR3KR cells and cluster 4 genes dex-regulated in both cell lines but whose expression differs. (**C**) The genes that were differently expressed between the cell lines were analyzed by IPA. The table shows the top six molecular and cellular functions that were the most significantly enriched for the genes differently expressed between wtGR and GR3KR cells. (**D**) RT-qPCR validation of genes that affect cell growth and are differently expressed between the cell lines. Bars represent the mean ± SD of three experiments. $^{***}P < 0.001$, $^{**}P < 0.01$ and $^{*}P < 0.05$ for the difference of dex treatment between wtGR- and GR3KR-expressing cells (Student's *t*-test).

SUMOylation modulates the GR activity on target genes regulating cellular grow.

To check whether the effect of GR SUMOylation on target gene expression is a feature unique to the HEK293 cells, we next examined the role of GR SUMOylation on gene expression in a different cell model, U2Os cells that have been previously used to study glucocorticoid signaling and post-translational modifications of the GR (10,13,44). We generated U2Os cell lines stably expressing wtGR or GR3KR and analyzed their genome-wide gene expression prolife in the presence and absence of dex. As with the HEK293 cell background, comparison of the dex-regulated genes between the U2Os-wtGR and the U2Os-GR3KR cells showed more dex-regulated genes in the SUMOylation-deficient U2Os GR-expressing cells (187 versus 159, respectively) (Supplementary Figure S3A). The dex-regulated genes in both cell lines were again grouped by unsupervised hierarchical clustering, resulting in six distinct clusters (clusters 1–6) (Supplementary Figure S3B). One gene from each cluster was validated by RT-qPCR (Supplementary Figure S4). IPA of the 160 genes that were differently expressed in the two U2Os cell lines revealed essentially the same molecular and cellular functions to be differently dex-regulated by the GR SUMOylation sites as in the HEK293 cells (Supplementary Figure S3C). RT-qPCR analyses of select dex-regulated genes that were differently expressed between the U2Os-wtGR and the U2Os-GR3KR cells and enriched in the latter cellular functions are shown in Supplementary Figure S3D. As in the HEK293 cells, *NFKBIA* was dex-regulated in both cell lines, but it had a significantly higher expression in the U2Os-wtGR cells than in the U2Os-GR3KR cells, whereas another well-known glucocorticoid responsive gene *SGK1* (45) showed a significantly higher expression in the U2Os-GR3KR cells than in the U2Os-wtGR cells. *IL8* and *PMEPA1* were dex-regulated only in the U2Os-wtGR cells and the U2Os-GR3KR cells, respectively. These results indicate that the regulatory effects of GR SUMOylation sites on GR target genes, such as the ones regulating cell growth, are not restricted to only one cell line.

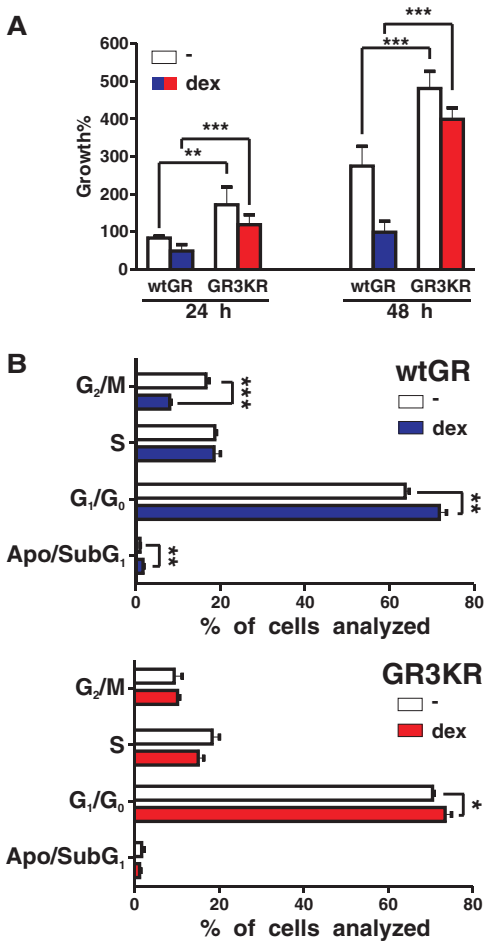

Figure 2. Cell proliferation and cell cycle distribution are affected by mutation of GR SUMOylation sites. (**A**) Cells were treated with dex as indicated and cell proliferation was measured by Cell Titer96 Aqueous cell proliferation assay reagent at the indicated time points. White bars depict vehicle-treated cells, blue bars dex-treated wtGR-expressing and red bars dex-treated GR3KR-expressing HEK293 cells. $***P < 0.001$ and $**P < 0.01$ for the difference between vehicle or dex treatment of wtGR- and GR3KR-expressing cells at indicated time points. (**B**) The wtGR- and GR3KR-expressing cells were exposed to vehicle or dex for 48 h and the proportion of cells in specific cell cycle phases was analyzed by FACS. $***P < 0.001$, $**P < 0.01$ and $*P < 0.05$ for the difference between vehicle and dex treatment for indicated cell cycle phase.

SUMOylation modulates the anti-proliferative effect of dex

Owing to the fact that the wtGR and the GR3KR cells showed significant differences in their dex-regulated expression of genes governing cellular proliferation and survival, we compared their growth rates and cell cycle distributions. As shown in Figure 2A, the GR3KR-expressing HEK293 cells proliferated significantly faster than their wtGR counterpart cells. Interestingly, also the anti-proliferative effect of dex was less pronounced in the GR3KR cells as compared with the wtGR cells; 48 h dex treatment had only a slight anti-proliferative effect on the GR3KR cells, but it markedly retarded the growth of the wtGR cells. The U2Os-GR3KR cells showed a similar trend of enhanced proliferation and attenuated response to dex treatment as the corresponding HEK293 cells (Supplementary Figure S3E). Additionally, according to FACS analyses, the dex exposure of the wtGR cells, but not that of the GR3KR cells, resulted in a significant decrease in the cells in G_2/M phase of the cell cycle (Figure 2B). Some of dex's anti-proliferative properties are because of its capability to induce apoptosis of certain cell types (46). Interestingly, dex treatment of the wtGR cells, but not that of the GR3KR cells, leads to a small but a significant increase in the amount of the cells in apo/subG_1 phase of the cell cycle, whereas no such effect was seen in the GR3KR cells. The anti-proliferative effects of dex on the proliferation of wtGR are thus reflected in the increase of cells in the apo/subG_1 and G_1/G_0 phase as well as the reduction of cells in G_2/M phase of the cell cycle, whereas in the case of the GR3KR cells, dex only affected the G_1/G_0 phase. In sum, our results indicate that the GR SUMOylation-associated differences in the

expression of growth regulatory genes are manifested in the growth of HEK293 cells.

SUMOylation influences genome-wide chromatin occupancy of the GR

To complement the GR target gene expression analyses, we next performed ChIPs with anti-GR antibody from wtGR and GR3KR HEK293 cells exposed to dex and sequenced the precipitated DNAs with Illumina HiSeq (ChIP-seq). The sequence reads of two biological replicates for the both cell lines were aligned to human reference hg19 genome by Bowtie, and MACS software was used to find significantly enriched peaks representing GRBs (cf. 'Materials and Methods' section). The ChIP-seq analyses revealed 11 255 and 18 856 high confidence GRBs in the wtGR and the GR3KR HEK293 cells, respectively. The mutation of the GR SUMOylation sites resulted in 8854 additional GRBs, whereas 1253 GRBs were lost and 10 002 GRBs remained unchanged (Figure 3A). However, the same classic GRE was found as the most enriched motif both in the wtGR unique and the GR3KR unique as well as the wtGR and GR3KR shared sites, when 1000 best-scoring GRBs for each group were analyzed (Figure 3C). At least one classic GRE was found in ~84 and 71% of the wtGR and GR3KR GRBs, respectively. In addition to the GREs, helix-loop-helix (HIF1A)- and E-twenty six (ETS) domain-binding motifs were found to be enriched in the GRBs unique to the GR3KR, and the shared GRBs additionally harbored homeodomain (SHOX2)-binding motifs. Interestingly, merely GREs were found in the wtGR unique GRBs. The overall distribution of the GRBs in relation to gene structures was practically the same in the wtGR and the GR3KR cells; most of the GRBs resided in introns or were intergenic (Figure 3B). In both cases, only ~10% of the GRBs were found within promoter regions (up to 10 kb upstream from transcription start sites, TSSs) and ~6% within 10 kb downstream from the gene. Of the genes whose expression was associated with dex regulation, i.e. altered by dex exposure, 58% in the wtGR cells and 69% the GR3KR cells showed at least one GRB ± 100 kb from their TSS. More upregulated genes than downregulated genes were associated with at least one GRB (Supplementary Figure S5A and B). The majority (~63%) of the GRBs associated with the dex-upregulated genes were shared between the wtGR and the GR3KR (Figure 3D), whereas the proportion of the shared GRBs was lower (~44%) among the dex-repressed genes (Figure 3E). Most of the GRBs associated with the dex-downregulated genes were intergenic, not intronic as in the case of the upregulated GR targets (Figure 3D and E). On average, there were more GRBs associated per one dex-up- and downregulated locus in the GR3KR cells compared with the wtGR cells, respectively. The difference in the number of the GRBs associated with the dex-upregulated genes between the wtGR and the GR3KR cells was significant ($P < 0.05$). Unique and shared GRBs of the dex-upregulated genes displayed at least one GRE per GRB, respectively, whereas in contrast to the wtGR unique GRBs of dex-repressed genes that showed no enrichment of full GREs, but only half GRE sites, the GR3KR unique GRBs displayed full GREs at a ratio of 1.8 GREs/GRB and enrichment of ETS domain-binding motifs (Figure 3G). The latter motif was also identified in the GR3KR unique GRBs, but not in the wtGR unique GRBs, of dex-activated genes (Figure 3F). Interestingly, no AP-1- or NF-κB-binding motifs were found to be enriched in the GRBs associated with the dex-repressed genes in the wtGR or the GR3KR cells.

Of the genes differently up- or downregulated by glucocorticoid because of the GR SUMOylation sites (i.e. genes that were dex-regulated in both cell lines but had a significant difference in their expression due to the GR SUMOylation sites), however, only a small number showed a GRB exclusively either in the wtGR cells (7 genes) or the GR3KR cells (86 genes) (Supplementary Figure S5E and F). Only one of the seven genes with the wtGR cell unique GRBs, the *CDKN1C*, was upregulated by dex, whereas the rest of them, *HOXC13, TSC22D1, CCND2*, *HOXA9*, *IL8* and *ZIC2*, were downregulated, with the repression of the latter four genes being significant only in the wtGR cells (Supplementary Figure S5E and F). Similarly, the majority (55/86) of the genes with the GR3KR unique GRBs were downregulated by dex with the majority of them being significantly downregulated only in the SUMOylation mutant GR cells (Supplementary Figure S5E and F).

Occupancy of SUMO-2/3 on the chromatin differs between the wtGR- and the GR3KR-expressing cells

We have recently shown evidence for co-occupancy of AR (highly related to the GR) and SUMO-2/3 on the chromatin of prostate cancer cells (27). Because SUMO-2 is the most abundant SUMO isoform in the HEK293 cells (data not shown) and the GR can be modified by SUMO-2/3 (Supplementary Figure S1B), we next performed ChIP-seq analyses with anti-SUMO-2/3 antibody from the wtGR- and the GR3KR-expressing HEK293 cells exposed to dex. The sequence reads of two biological replicates were analyzed in the same way as the GR data to find out whether there are significantly enriched peaks representing SUMO-2/3-enriched binding sites (SUMOBs). Interestingly, these genome-wide analyses revealed that SUMO-2/3 is enriched at 12 109 and 7753 high confidence SUMOBs in the wtGR and the GR3KR cells, respectively. Mutation of the GR SUMOylation sites associated with a loss of 6329 SUMOBs and an appearance of 1973 new SUMOBs, whereas 5780 SUMOBs remained unchanged (Figure 4A). Comparison of the overlap between the GRBs and the SUMOBs showed ~38% co-occupancy in the wtGR cells (Figure 5A) and ~16% co-occupancy in the GR3KR cells (Figure 5B). The GRE was found in the SUMOBs unique to the wtGR as well as in the SUMOBs shared between the wtGR and the GR3KR, but only a homeodomain (PAX6)-binding motif was found in the SUMOBs unique to the GR3KR, when 1000 best-scoring SUMOBs for each group were analyzed (Figure 4C). In addition to the classic GRE, the SUMOBs unique to the wtGR showed enrichment of

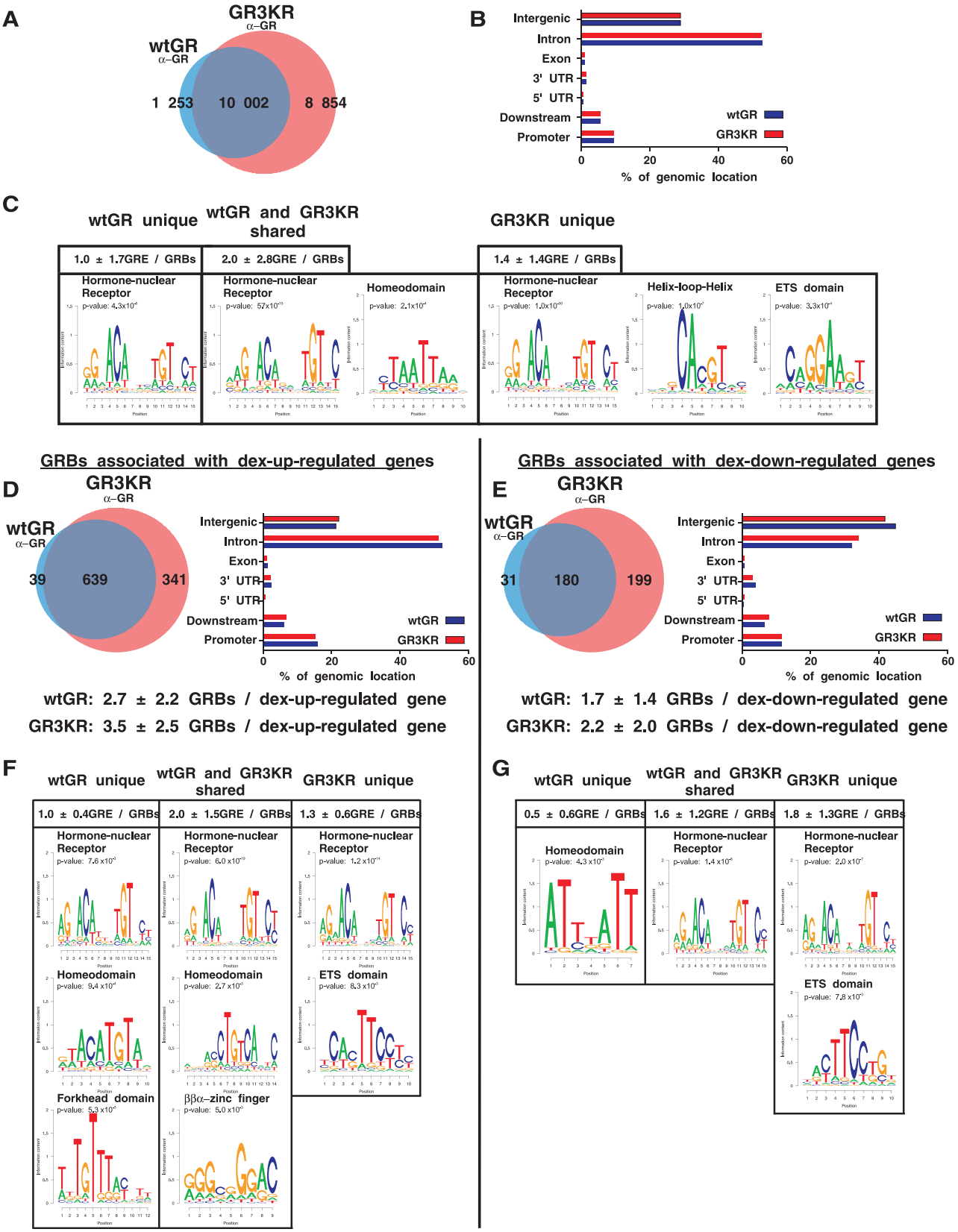

Figure 3. Genome-wide occupancy of the GR in chromatin is influenced by the receptor's SUMOylation sites. The wtGR- and GR3KR-expressing HEK293 cells were exposed for dex for 1 h, and ChIP-seq of anti-GR antibody-precipitated samples was performed using Illumina HiSeq System as described in 'Materials and Methods' section. Obtained sequence reads were aligned to human reference genome by using Bowtie and significantly enriched peaks that represent GRBs were detected using MACS as described in 'Materials and Methods' section. (**A**) Venn-diagram showing comparison of the GRBs between the wtGR- (blue) and the GR3KR-expressing cells (red). Values inside the diagram indicate the number of

(continued)

ββα-zinc finger (ZFP410)-binding motif. The overall distribution of SUMOBs in relation to gene structures was practically the same in the wtGR and the GR3KR cells (Figure 4B) and similar to that of the GRBs. However, clearly more SUMOBs than the GRBs, ~21 versus 10%, were found at the promoter regions (cf. Figure 3B versus Figure 4B).

Of the genes whose expression was altered by dex, 55% in the wtGR cells and 47% in the GR3KR cells showed at least one SUMOB ± 100 kb from their TSS. More upregulated genes than downregulated genes were associated with at least one SUMOB (Supplementary Figure S6A and B). Over half of the GRBs associated with the dex-upregulated genes in the wtGR cells overlapped with the SUMOBs (Figure 5C), whereas less than one-third in the GR3KR did so (Figure 5D). For the dex-downregulated genes, the co-occupancy percentages were generally lower (Figure 5E and F). On average, there were more SUMOBs associated per one dex-up- and downregulated locus in the wtGR cells compared with the GR3KR cells, respectively. The difference in the number of the SUMOBs associated with the dex-upregulated genes between the wtGR and the GR3KR cells was significant ($P < 0.05$). Also, when related to the number of GRBs per dexregulated locus, there were on average more SUMOBs in the wtGR than in the GR3KR cells (Figure 4D and E). As with the GRBs, only a small number of genes showed a SUMOB exclusively in the wtGR cells (83 genes) or the GR3KR cells (28 genes) (Supplementary Figure S6E and F). The GRE and a leucine zipper (JUND)-binding motif were found to be enriched merely among the wtGR unique SUMOBs, whereas an NR2-type nuclear receptor motif was enriched at the wtGR and the GR3KR shared SUMOBs, and no motif was enriched at the GR3KR unique SUMOBs associated with the dex-up-regulated loci (Figure 4F). Interestingly, the GRE was not enriched among the SUMOBs associated with dex-downregulated loci (Figure 4G).

Comparison of the GRBs and the SUMOBs associated with dex-regulated genes between the wtGR and the GR3KR cells also indicated that the majority (~77%) of the sites that contain both the GRBs and the SUMOBs in the wtGR cells, but merely the GRBs in the GR3KR cells, are associated with genes that are differently regulated between these cells, such as *NFKBIA*, *RASD1* and *MAFB* (Figure 5G and H). Moreover, most of the unique or the shared GRBs in the wtGR and the GR3KR cells without SUMOBs were differently dex-regulated between these cells. Interestingly, the ETS-domain motif was found to be enriched at the GR3KR unique GRBs without SUMOBs (Supplementary Figure S7A and B).

GR occupancy in loci regulating cellular growth is sensitive to SUMOylation

Although on the whole genome level, the majority of the GRBs were insensitive to the GR SUMOylation sites, inspection of the ChIP-seq data revealed reproducible and clear differences between the wtGR and the GR3KR chromatin occupancy of genes linked to cellular growth and survival pathways. For example, the differences in the GR occupancy of the growth regulatory genes analyzed in Figure 1D paralleled with their gene expression levels. At the *CDKN1C* locus (Figure 6A), there was a significant GRB ~5 kb upstream from the TSS only in the wtGR cells. At the *NFKBIA* locus (Figure 6B), the enrichment of GR in the GRBs closest to the *NFKBIA* was clearly higher in the wtGR cells. The situation was similar at the *MAFB* locus (Figure 6F). The intronic sites of *ELK1* (Figure 6C) contained two GRBs in the GR3KR cells but only one in the wtGR cells that had a lower GR occupancy than its counterpart in the GR3KR cells. Similarly, the GR occupancy at the *MERTK* locus and that at the *RASD1* were higher in the GR3KR cell locus (Figure 6D and E). Interestingly, the binding of SUMO-2/3 to the *NFKBIA*, the *ELK1*, the *RASD1* and the *MAFB* overlapped with that of wtGR, whereas only the strongest GRBs in the *NFKBIA*, *ELK1* and *MAFB* loci showed binding of both SUMO-2/3 and GR3KR, and the SUMO-2/3 binding to these sites was clearly weaker than with the wtGR. Re-ChIP assays in which chromatin was sequentially immunoprecipitated with anti-SUMO-2/3 and anti-GR antibody confirmed the simultaneous presence of the SUMO-2/3 and the GR at the two *RASD1* regulatory regions (cf. Figure 6E) and at the one *MAFB* regulatory region (cf. Figure 6F) in the wtGR cells but not in the GR3KR cells (Figure 7). These results strongly suggest that chromatin-bound GR can be conjugated by SUMO-2/3. The GR chromatin occupancy of dex-repressed genes was also sensitive to GR SUMOylation. Examples of the GR chromatin occupancy in the loci whose expression was differentially dex-repressed between the wtGR and the GR3KR cells (Supplementary Figure S8) are shown in Figure 8. For example, *CXXC4*, *DMRT3* and *SPRY1* displayed higher chromatin occupancy by GR3KR than wtGR, which also paralleled with the differential ability of these two receptor

Figure 3. Continued
GRBs shared and unique to each cell line. (**B**) Enrichment of GRBs to different genomic locations was analyzed by CEAS tool in Cistrome. Promoter region encompasses 10 kb area upstream of gene TSSs and downstream region 10 kb area downstream of gene. (**C**) Top motifs from 1000 best-scoring GRBs by fold enrichment from the following sets; GRBs unique to wtGR, GRBs unique to GR3KR and GRBs common to both wtGR and GR3KR were analyzed with SeqPos tool in Cistrome. The mean ± SD of the number of GREs found in one GRB and the *P*-values of the motif enrichment are shown. (**D**) Venn-diagram showing comparison of the GRBs associated with the dex-upregulated genes between the wtGR (blue) and the GR3KR cells (red). Values inside the diagram indicate the number of GRBs shared and unique to each cell line. Enrichment of GRBs to different genomic locations was analyzed by CEAS tool in Cistrome. (**E**) The same analyses as in (D) but for GRBs associated with the dex-downregulated genes. (**F**) Motif enrichment of the GRBs associated with dex-upregulated genes (GRBs unique to the wtGR, GRBs unique to the GR3KR and GRBs common to both the wtGR and the GR3KR) was analyzed with SeqPos tool in Cistrome. The mean ± SD of the number of GREs found in one GRB and the *P*-values of the motif enrichment are shown. (**G**) The same analyses as in (F) but for GRBs associated with dex-downregulated genes.

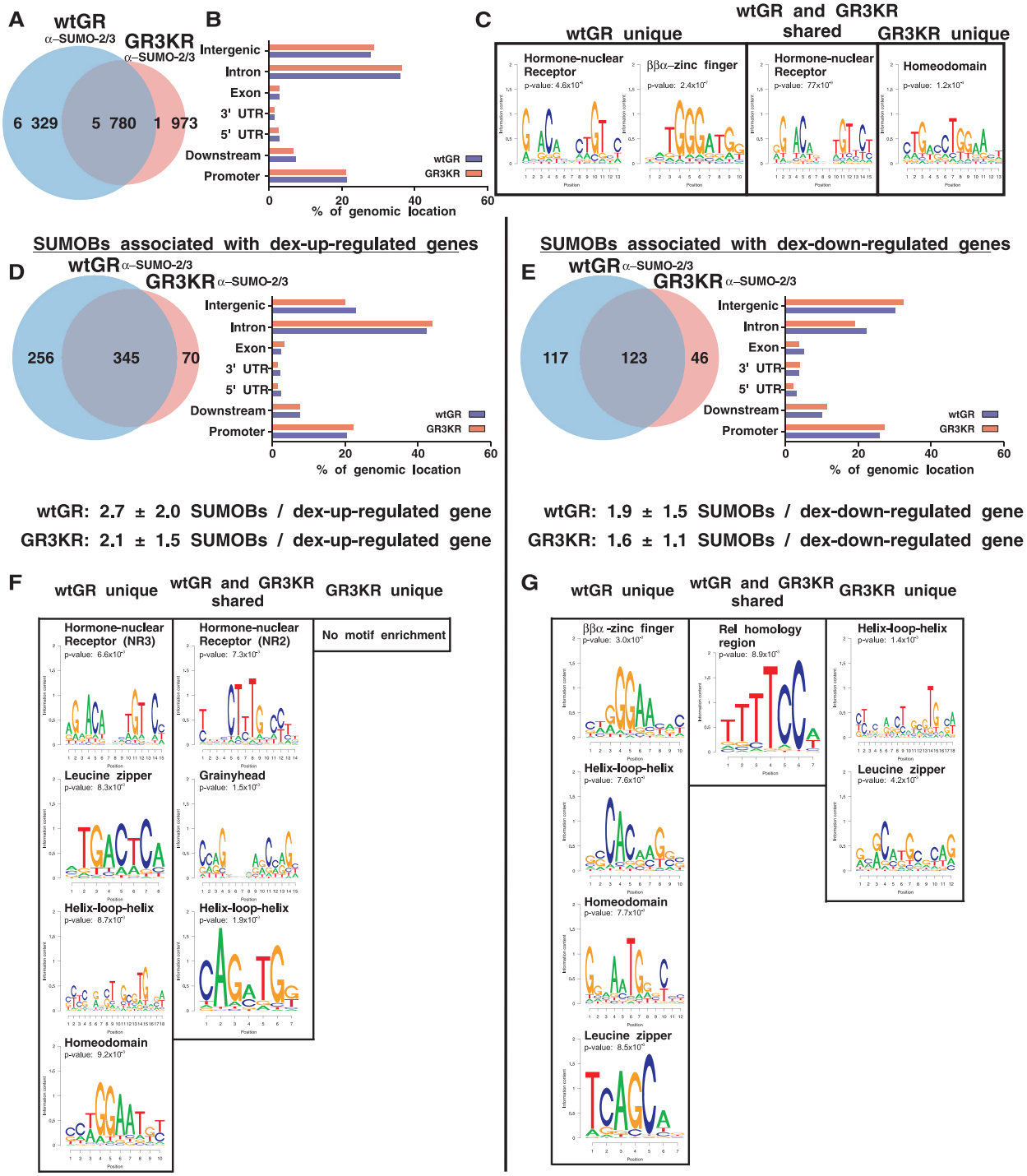

Figure 4. The genome-wide occurrence of SUMO-2/3 chromatin marks differs between the wtGR- and GR3KR-expressing cells. The wtGR- and GR3KR-expressing HEK293 cells were exposed for dex for 1 h, and ChIP-seq of anti-SUMO-2/3 antibody-precipitated samples was performed using Illumina HiSeq System as described in 'Materials and Methods' section. Obtained sequence reads were aligned to human reference genome by using Bowtie and significantly enriched peaks that represent SUMO-2/3-binding sites (SUMOBs) were detected using MACS cf. 'Materials and Methods' section. (**A**) Venn diagram showing comparison of the SUMOBs between the wtGR- (light blue) and the GR3KR cells (light red). Values inside the diagram indicate the number of SUMOBs shared and unique to each cell line. (**B**) Enrichment of SUMOBs to different genomic locations was analyzed by CEAS tool in Cistrome. (**C**) Top motifs from 1000 best-scoring GRBs by fold enrichment from the following sets; SUMOBs unique to the wtGR, SUMOBs unique to the GR3KR and SUMOBs common to both the wtGR and the GR3KR were analyzed with SeqPos tool in Cistrome. (**D**) Venn diagram showing comparison of the SUMOBs associated with the dex-upregulated genes between the wtGR (light blue) and the GR3KR cells (light red). Values inside the diagram indicate the number of SUMOBs shared and unique to each cell line. Enrichment of SUMOBs to different genomic locations was analyzed by CEAS tool in Cistrome. The mean ± SD of the number of SUMOBs for each dex-upregulated gene is shown. (**E**) The same analyses as in (D) but for SUMOBs associated with dex-downregulated genes. (**F**) Motif enrichment of the SUMOBs associated with dex-upregulated from the following sets; SUMOBs unique to the wtGR, SUMOBs unique to the GR3KR and SUMOBs common to both the wtGR and the GR3KR were analyzed with SeqPos tool in Cistrome. (**G**) The same analyses as in (F) but for SUMOBs associated with dex-downregulated genes. The *P*-values of the motif enrichment are shown.

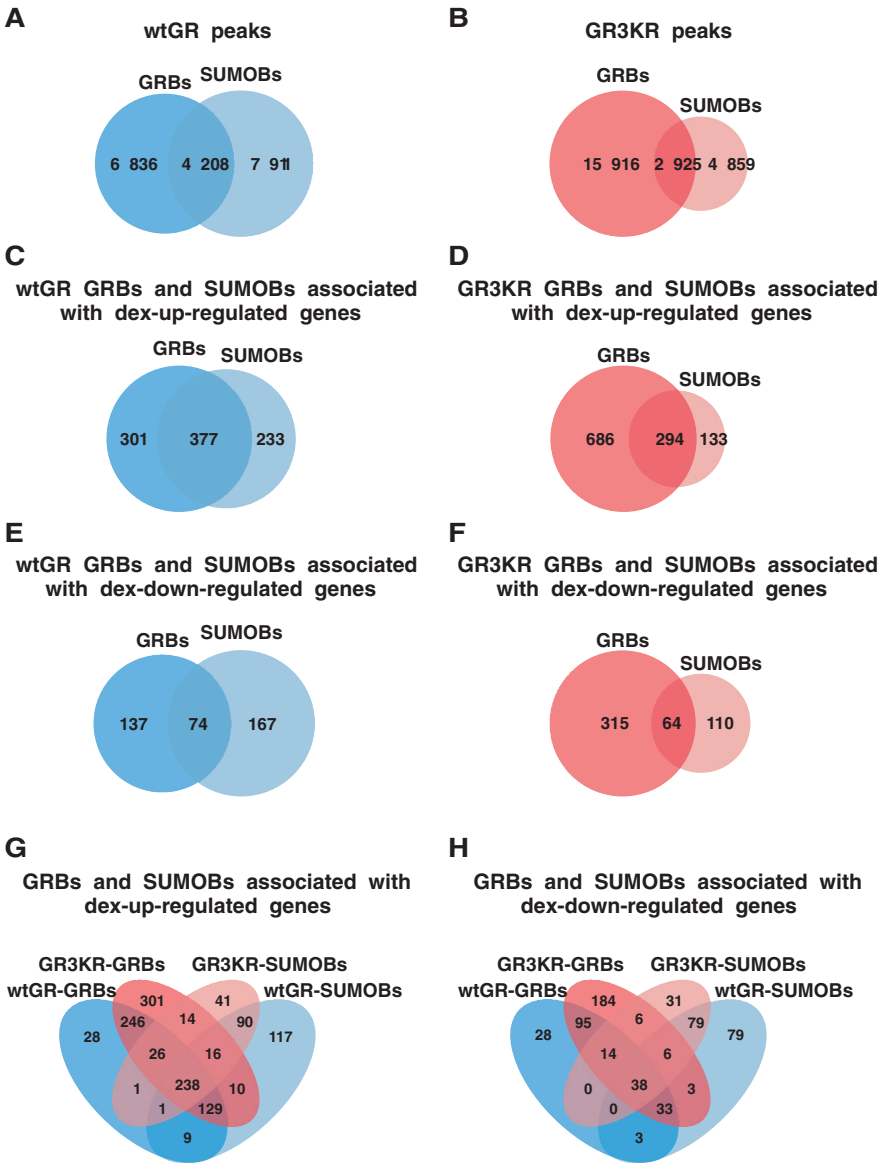

Figure 5. Comparison of GRBs and SUMOBs in the wtGR- and the GR3KR-expressing cells. (**A** and **B**) Venn diagrams showing comparison of the GRBs and the SUMOBs between the wtGR and the GR3KR HEK293 cells. (**C** and **D**) Venn diagrams showing comparison of the GRBs and the SUMOBs associated with dex-upregulated genes. (**E** and **F**) Venn diagrams showing comparison of the GRBs and the SUMOBs associated with dex-downregulated genes. Values inside the diagram indicate the number shared and unique GRBs and SUMOBs. (**G**) The quadruple Venn diagram shows the comparison between GRBs (blue/red) and SUMOBs (light blue/red) associated with dex-upregulated genes between wtGR- and GR3KR-expressing cells. Values inside the diagram indicate the unique GRBs and SUMOBs to each cell line and the different intersections of GRBs and SUMOBs between each other and between each cell line. (**H**) The same analysis as in (G) but for GRBs and SUMOBs associated with dex-downregulated genes.

forms to repress these genes. In the case of *CCND2*, *IL8* and *ZIC2*, the situation was converse, but with regard to the GR occupancy, the differences were less dramatic. However, the SUMO-2/3 binding to these loci was generally low in comparison with the examples of dex-upregulated genes sensitive to GR SUMOylation.

DISCUSSION

SUMOylation has emerged as an important regulatory modification of transcription factors, including nuclear receptors (47). SUMOylations have been often linked to transcriptional repression (15,48). However, the effects of SUMO modifications on transcription factor function and targets have only in rare cases been addressed in a systematic genome-wide fashion. In this work, we have used genome-wide approaches to investigate how SUMOylation sites of the GR influence endogenous target gene expression and GR chromatin occupancy by using isogenic HEK293 cell models expressing either the wtGR or the SUMOylation-defective GR. Analysis of genes differentially regulated by the wtGR and the GR SUMOylation mutant indicated that the SUMOylation sites do not simply repress the GR activity on all target

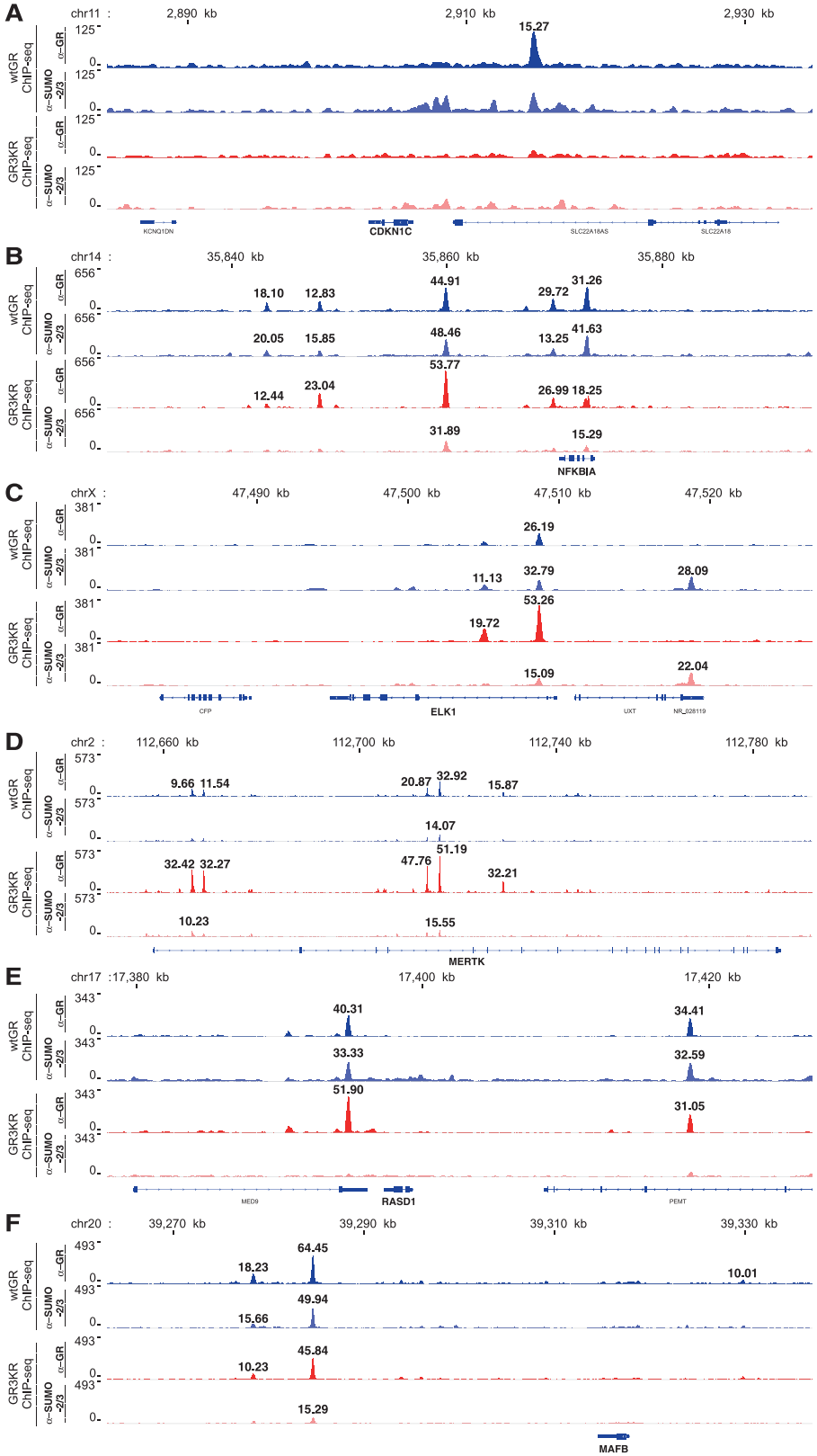

Figure 6. Examples of dex-regulated cell growth-associated gene loci in which binding of GR and SUMO-2/3 differs between the wtGR- and the GR3KR-expressing cells. (**A–F**) Peak tracts showing the occupancy of GR and that of SUMO-2/3 in the regulatory regions of *CDKN1C* (A), *NFKBIA* (B), *ELK1* (C), *MERTK* (D), *RASD1* (E) and *MAFB* (F). Blue track represents ChIP-seq with anti-GR antibody and light blue track represents ChIP-seq with anti-SUMO-2/3 antibody in wtGR-expressing cells. Red track represents ChIP-seq with anti-GR antibody and light red track represents ChIP-seq with anti-SUMO-2/3 antibody in GR3KR-expressing cells. The numbers above the GRBs and SUMOBs depict the fold enrichment (FE) value. The GRBs and the SUMOBs in the peak tracks marked with the FE values were found in the two biological replicates. Binding of GR by ChIP-seq in the control FRT cells to the same loci is shown in Supplementary Figure S9.

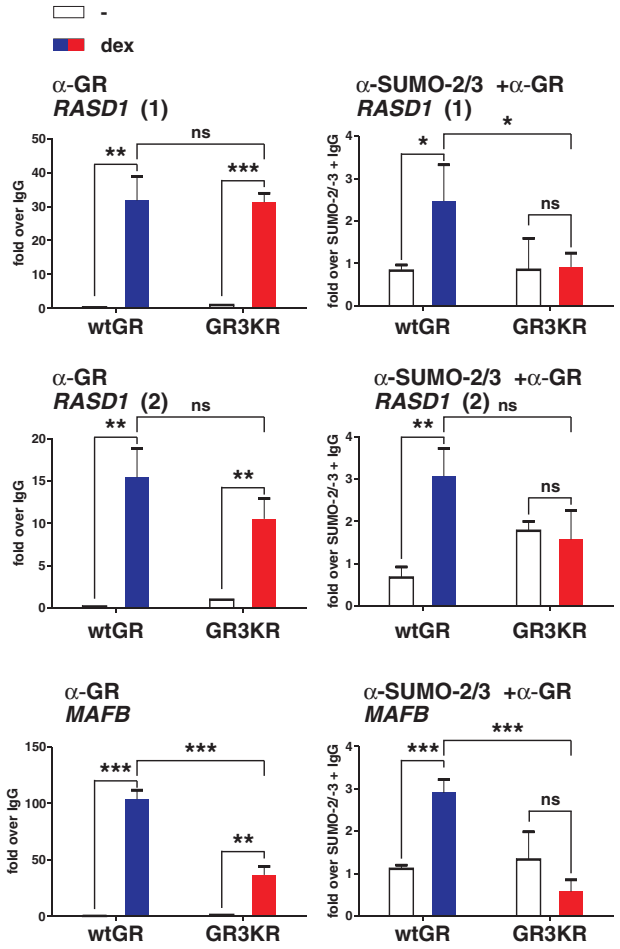

Figure 7. GR binds to the regulatory regions of *RASD1* and *MAFB* similarly in the wtGR- and the GR3KR-expressing cells, but only in the wtGR-expressing cells a significant portion of the chromatin bound GR is SUMO-2/3-modified. (Left panels) Occupancy of GR in *RASD1* [*RASD1* (1); 2.5 kb 5′ from TSS, *RASD1* (2); 21 kb 3′ from TSS] and *MAFB* (36 kb 5′ from TSS) regulatory regions after 1 h exposure to dex were monitored using qChIP with anti-GR antibody (left panel). Results are shown as fold over to the normal IgG-precipitated samples. (Right panels) The same chromatin regions were analyzed by re-ChIP assays in which chromatin was sequentially immunoprecipitated with anti-SUMO-2/3 and anti-GR antibody. Results are shown as fold over to control re-ChIP assays in which normal IgG was used instead of the anti-GR antibody. Blue bars depict dex-treated wtGR-expressing cells and red bars dex-treated GR3KR-expressing cells and results represent the mean ± SD of three experiments. ***$P < 0.001$; **$P < 0.01$ and *$P < 0.05$ (Student's *t*-test) for the difference of vehicle and dex treatment in either wtGR- or GR3KR-expressing cells or for the difference of dex treatment between wtGR- and GR3KR -expressing cells. ns, no significance.

genes; the mutant exhibited differential, also attenuated transcriptional activity, but not on all the target genes. SUMOylation not merely affected the expression of dex-induced genes, but it also influenced the ability of GR to repress its target genes. Interestingly, IPA revealed that the differently expressed genes were significantly associated with molecular and cellular functions of gene expression, development, movement, growth and proliferation, cell death and survival and cell cycle. Many genes, such as *CDKN1C* and *NFKBIA*, that have anti-proliferative effects showed significantly stronger dex-upregulation by the wtGR. The *CDKN1C* encodes a cyclin-dependent kinase inhibitor p57 that inhibits cell proliferation by accumulating cells in the G_1 phase of the cell cycle (43,49,50). The *NFKBIA* has an anti-proliferative effect due to its protein product IκBα's ability of restrict the action of NF-κB (6,8). On the other hand, genes, such as *ELK1* and *RASD1*, that were more robustly upregulated by the SUMOylation-deficient GR are associated with promotion of cell proliferation. ELK1 is an ETS transcription factor family member and regulated by the RAS-RAF-MAPK signaling. It interacts with the serum response factor and the serum response element in the *c-FOS* promoter (51,52). The *RASD1*, a member of the RAS superfamily, may play a role in dex-induced alterations in cell morphology, growth and cell-extracellular matrix interactions (53).

The GR SUMOylation sites affected essentially the same molecular and cellular programs in our other cell model, U2Os cells as in the HEK293 cells. The *NFKBIA* was expressed at a significantly higher level in also dex-exposed wtGR-expressing U2Os cells. As expected, there were also cell-specific differences in the expression of certain target genes, such as *IL8*, a proinflammatory chemokine (54) that was upregulated in the wtGR U2Os cells, but unaffected by dex in the GR3KR U2Os cells, whereas in the corresponding HEK293 cell model, the gene was significantly downregulated by dex, but only in the wtGR cells. On the other hand, *PMEPA1*, that has been shown to confer cell growth inhibition in AR positive prostate cancer cells (55), was dex-downregulated only in GR3KR U2Os cells.

SUMOylation also influenced the GR cistrome. On the whole genome-wide level, the mutation of the GR SUMOylation sites yielded seven times more GRBs than were lost, albeit the majority of them were not affected by the mutation. However, the genomic location distribution of the GRBs remained essentially unaffected by the mutation of GR SUMOylation sites. In the both cell models, more than half (~52%) of the GRBs resided in introns, whereas promoter regions (up to 10 kb upstream from TSSs) harbored only ~10% of the GRBs. These genomic distribution figures are similar to those of the GRBs recently reported from HeLa B2 cells, mouse primary bone marrow-derived macrophages and mouse mammary 3134 adenocarcinoma cells (56–58). The classical GRE that was also identified in these ChIP-seq analyses (56–59) was the prevalent motif found in our model HEK293 cells.

The dex-upregulated genes in both cell models contained more commonly at least one GRB than the downregulated genes (the wtGR cells: 73 versus 43%; the GR3KR cells: 79 versus 58%, respectively), suggesting that the dex-induced gene activation is more commonly associated to direct binding of holo-GR to the target locus than the gene repression. Also the average numbers of GRBs per dex-regulated locus were higher for the dex-activated genes than for the dex-repressed genes, with the numbers being 2.7 versus 1.7 for the wtGR and 3.5 versus 2.2 for the GR3KR, respectively. However, comparison of motif signatures within gene

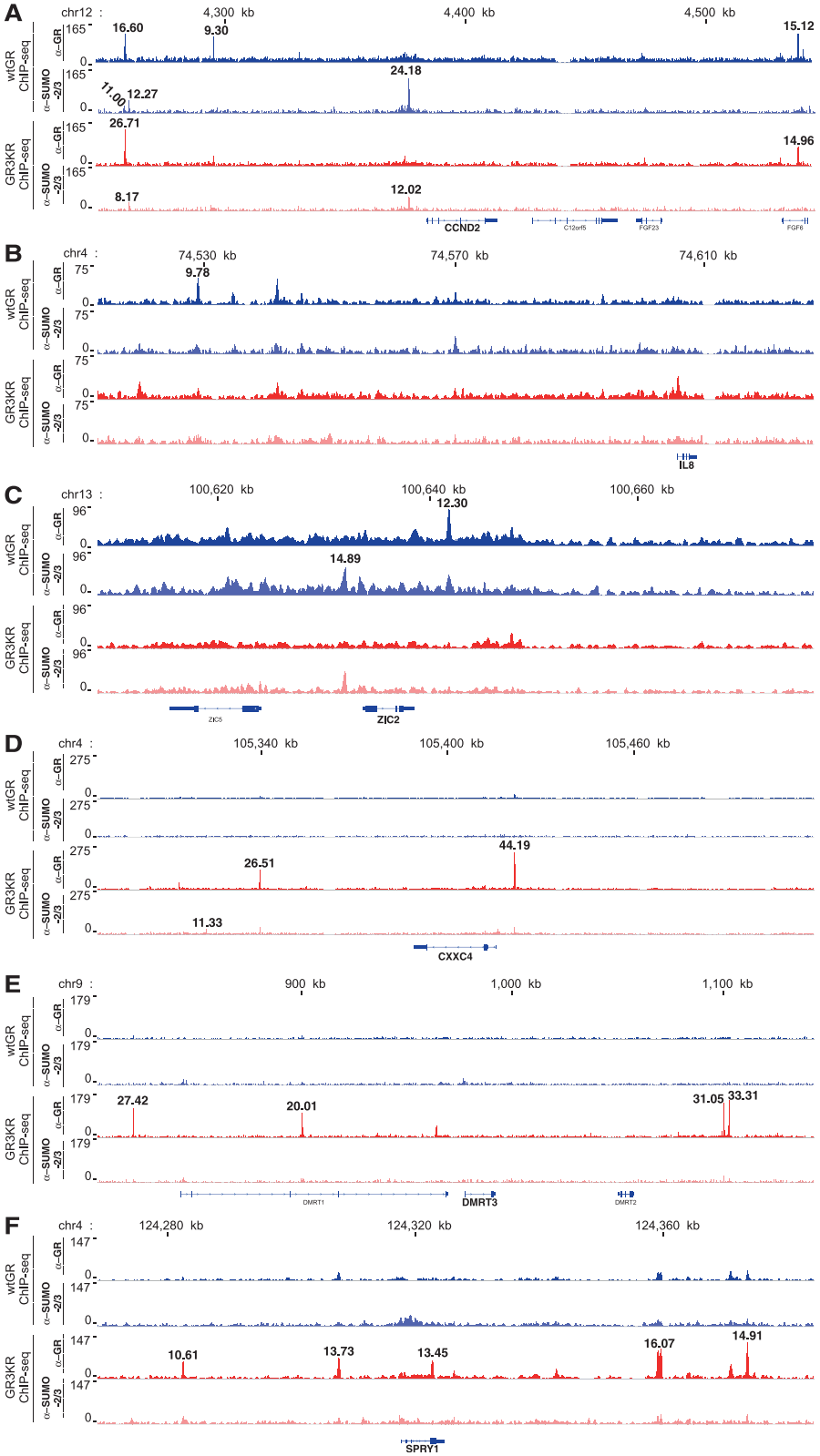

Figure 8. GR and SUMO-2/3 occupancy in select dex-downregulated genes differentially expressed between wtGR and GR3KR cells and associated with unique GRBs. (**A–F**) Peak tracts showing the occupancy of GR and that of SUMO-2/3 in the regulatory regions of *CCND2* (A), *IL8* (B), *ZIC2* (C) that are dex-downregulated in wtGR-expressing cells, and *CXXC4* (D), *DMRT3* (E) and *SPRY1* (F) that are dex-downregulated in GR3KR-expressing cells. Blue track represents ChIP-seq with anti-GR antibody and light blue track represents ChIP-seq with anti-SUMO-2/3 antibody in wtGR-expressing cells. Red track represents ChIP-seq with anti-GR antibody and light red track represents ChIP-seq with anti-SUMO-2/3 antibody in GR3KR-expressing cells. The numbers above the GRBs and the SUMOBs depict the fold enrichment (FE) value. The GRBs and the SUMOBs in the peak tracks marked with the FE values were found in the two biological replicates. The binding of GR by ChIP-seq in control FRT cells to the same loci is shown in Supplementary Figure S10.

repression- and activation-associated GRBs revealed remarkably similar features and the presence of GREs in both cases, which was recently also noted by Uhlenhaut and co-workers (57), suggesting that the GR binding to GREs commonly mediates the gene repression. This notion contrasts with previous ideas based on a relatively small number of model target gene promoters, that mainly tethering of GR to AP-1 or NF-κB is responsible for the repression of transcription by glucocorticoids (6). Interestingly, most of the GR SUMOylation-modulated GRBs were associated with genes that were downregulated by dex.

It is of note, however, that of the all dex-regulated loci associated with at least one GRB within 100 up- or downstream the gene (462 loci), only a minor portion was exclusively occupied by the wtGR (7 loci) or the SUMOylation-deficient GR (86 loci). More typically than having unique GRBs, GR target loci differentially regulated because of the GR SUMOylation sites, such as the *NFKBIA*, the *ELK1* and the *RASD1*, associated with cell proliferation, showed differences in their number of GRBs and/or in the level of GRB receptor occupancy between the wtGR and the GR3KR cells. Generally, the level of receptor occupancy in a given locus correlated with the glucocorticoid-responsiveness of gene expression of the locus. This was seen both in the case of gene induction and repression. The cells expressing SUMOylation mutant GR proliferated more rapidly and their anti-proliferative response to dex was less pronounced than in the wtGR-expressing cells. The difference was associated with the altered regulation and GR chromatin occupancy of several genes influencing cell growth. Interestingly, also in the case of progesterone receptor (PR), SUMOylation was recently reported to regulate PR target gene selection in breast cancer cells, and again the SUMO sensitive PR target genes included genes required for proliferative and pro-survival signaling, which was reflected in the growth of these cells (60). Indirect effects caused by the long-term expression of different forms of PR and GR may to a small extent have differently programed the cells, which may have also contributed to their growth characteristics. Similarly, SUMOylation-defective microphthalmia-associated transcription factor (MITF) mutant that is associated to predisposition to melanoma and renal carcinoma clearly differed from its wild-type counterpart on some, but not all, MITF target genes, with the subset of genes affected being related to cell growth and proliferation (61). As with the GR, the SUMOylation site mutation influenced the MITF's chromatin occupancy (61). Mutation of the SUMOylation sites in GATA-1 in turn considerably attenuated its capability to induce several genes controlling hematopoiesis, and the attenuated activity was linked to decreased chromatin occupancy (62). Moreover, elimination of orphan nuclear receptor SF-1 (steroidogenic factor 1) SUMOylation in mice resulted in abnormal Hedgehog signaling and endocrine development (63). The abnormalities seemed to be linked to altered recognition of a group of target genes sensitive to the modification of SF-1 (63). These results together indicate that SUMOylation can regulate target gene selection of sequence-specific transcription factors, at least in part by influencing chromatin occupancy of transcription factors.

Our ChIP-seq data also revealed the occurrence of SUMO-2/3 in the chromatin and its enrichment to gene regulatory regions. Overall, the chromatin distribution of SUMO-2/3 peaks in the GR-expressing HEK293 cells resembled that of the GRs peaks, with the majority of the peaks being at intergenic or intronic regions. The occurrence of SUMO-2/3 in the promoter regions, however, was more prominent than that of GR. Comparison of the overlap between the GR binding and the SUMO-2/3 marks showed a markedly better (2-fold higher) overlap in the SUMOylation competent GR than in the modification deficient GR-expressing cells. This difference and results from sequential ChIP assays imply that SUMOylated GR is capable of interacting with the chromatin. Furthermore, the GRE was found to be enriched merely among the wtGR cell unique SUMO-2/3-binding sites of the dex-regulated loci, whereas no sequence motif enriched at the GR3KR unique SUMO-2/3-binding sites. However, because the SUMO-2/3 was still found to co-occupy a large number of sites with the SUMOylation deficient GR, the chromatin co-occupancy does not solely derive from the SUMOylated GR, but also from other chromatin-interacting proteins, transcription factors or coregulators, that can be modified by SUMOs. The occurrence of chromatin SUMO-2/3 marks in relation to the GR-binding enhancers and the promoters of dex-regulated genes in our model HEK293 cells compared with the cell background (without added GR, data not shown) indicates that the chromatin-bound SUMO-2/3 is associated with transcriptionally active chromatin and playing a dynamic role in the modulation of GR function on the chromatin. Additionally, comparison of the ENCODE DNase-seq data set from HEK293T cells with our data sets indicates $\geq$30 and 45% overlap with the SUMO-2/3 + GR peaks and the SUMO-2/3 − GR peaks, respectively, with the DNaseI hypersensitive chromatin sites, i.e. 'open' chromatin regions (Supplementary Figure S11). The ENCODE HEK293 cell H3K4me3 data set showed also $\geq$30% overlap with the SUMO-2/3 − GR peaks, whereas the overlap with the SUMO-2/3 + GR peaks was $<$10%, possibly reflecting the differential enrichment of the histone mark and the GR at promoter regions (Supplementary Figure S11). While this article was under review, a genome-wide study from WI38 human fibroblast revealed that SUMO-2/3 and SUMOylation machinery are enriched at the histone and transfer RNA gene clusters (64). Interestingly, this enrichment is not restricted to the fibroblasts, as a similar SUMO-2/3 enrichment is visible at the same gene clusters in our HEK293 model cells (data not shown). Otherwise, however, less than one-third of the SUMO-2/3 peaks in the wtGR HEK293 cells (32% in vehicle- and 30% dex-exposed cells) overlap with those in the WI38 cells. Interestingly, binding motif analyses of the GRBs indicated, in addition to the GREs, enrichment ETS domain-binding motifs among the GR3KR unique GRBs associated with dex-up- and dex-downregulated genes. Unfortunately, the *in silico* analyses cannot differentiate between the ETS family proteins and able to

predict the most likely binding candidate, as the DNA-binding specificities of the family members are highly similar (65). The motif analyses suggest that SUMOylation may influence the GR chromatin occupancy and target gene selection via regulating interactions with other sequence-specific transcription factors, such as ETS proteins, which may promote or prevent the GR binding to the chromatin. The average number of GREs among the GRBs that were unique to the SUMOylation mutant GR was also somewhat higher than that among the wtGR unique GRBs. Inspection of the GRBs associated with the dex-repressed genes revealed enrichment of full GREs (1.8 GREs/GRB) among the GR3KR unique GRBs, whereas only half sites of GREs were present among the wtGR unique GRBs. Thus, our results also hint at the possibility that GRB signature, or number of GRE within the binding sites, contributes to the SUMOylation-regulated binding of GR to its DNA targets. This notion is reminiscent of the synergy control motif concept in which SUMOylation-mediated regulation of GR's synergistic activity depends on stable interaction with DNA (29). SUMOylation-mediated synergy control may also involve local changes in histone marks and chromatin signature (66). In conclusion, our objective genome-wide analyses reveal that SUMOylation does not simply repress the GR activity, but the modification regulates the receptor's target gene selection and it plays an important role in controlling the anti-proliferative effect of glucocorticoids.

ACCESSION NUMBERS

Bead array and ChIP-seq data is submitted to the NCBI Gene Expression Omnibus database (http://www.ncbi.nlm.nih.gov/geo/), accession code: GSE48379.

SUPPLEMENTARY DATA

Supplementary Data are available at NAR Online

ACKNOWLEDGEMENTS

The authors thank Merja Räsänen and Eija Korhonen for assistance with cell cultures, Antti Ropponen for guidance in the FACS analyses and Merja Heinäniemi and Sami Heikkinen for their help with the construction of deep sequencing pipeline. The EMBL GeneCore sequencing team and the Finnish Microarray and Sequencing Centre are also greatly acknowledged for deep sequencing and microarray analyses.

FUNDING

The Academy of Finland, the Finnish Cancer Organizations, the Emil Aaltonen Foundation, UEF Doctoral Programme in Molecular Medicine and the Sigrid Jusélius Foundation. Funding for open access charge: The Academy of Finland.

Conflict of interest statement. None declared.

REFERENCES

1. Heitzer,M.D., Wolf,I.M., Sanchez,E.R., Witchel,S.F. and DeFranco,D.B. (2007) Glucocorticoid receptor physiology. *Rev. Endocr. Metab. Disord.*, **8**, 321–330.
2. Barnes,P.J. (1998) Anti-inflammatory actions of glucocorticoids: molecular mechanisms. *Clin. Sci. (Lond).*, **94**, 557–572.
3. Rosenfeld,M.G., Lunyak,V.V. and Glass,C.K. (2006) Sensors and signals: a coactivator/corepressor/epigenetic code for intergrating signal-dependent programs of transcriptional response. *Genes Dev.*, **20**, 1405–1428.
4. Biddie,S.C., John,S., Sabo,P.J., Thurman,R.E., Johnson,T.A., Schiltz,R.L., Miranda,T.B., Sung,M.-H., Trump,S., Lightman,S.L. *et al.* (2011) Transcription factor AP1 potentiates chromatin accessibility and glucocorticoid receptor binding. *Mol. Cell*, **43**, 145–155.
5. John,S., Sabo,P.J., Johnson,T.A., Sung,M.-H., Biddie,S.C., Lightman,S.L., Voss,T.C., Davis,S.R., Meltzer,P.S., Stamatoyannopoulos,J.A. *et al.* (2008) Interaction of the glucocorticoid receptor with the chromatin landscape. *Mol. Cell*, **29**, 611–624.
6. De Bosscher,K., Berghe,W.V. and Haegeman,G. (2003) The interplay between the glucocorticoid receptor and nuclear factor-kB or activator protein-1: molecular mechanisms for gene repression. *Endocr. Rev.*, **24**, 488–522.
7. Smoak,K.A. and Cidlowski,J.A. (2004) Mechanisms of glucocorticoid receptor signalling during inflammation. *Mech. Ageing Dev.*, **125**, 697–706.
8. Vallabhapurapu,S. and Karin,M. (2009) Regulation and function of NF-κB transcription factors in the immune system. *Annu. Rev. Immunol.*, **27**, 693–733.
9. Viegas,L.R., Hoijman,E., Beato,M. and Pecci,A. (2008) Mechanisms involved in tissue-specific apoptosis regulated by glucocorticoids. *J. Steroid Biochem. Mol. Biol.*, **109**, 273–278.
10. Rogatsky,I., Trowbridge,J.M. and Garabedian,M.J. (1997) Glucocorticoid receptor-mediated cell cycle arrest is achieved through distinct cell-specific transcriptional regulatory mechanisms. *Mol. Cell Biol.*, **17**, 3181–3193.
11. Tian,S., Poukka,H., Palvimo,J.J. and Jänne,O.A. (2002) Small ubiuitin-related modifier-1 (SUMO-1) modification of the glucocorticoid receptor. *Biochem. J.*, **367**, 907–911.
12. Galliher-Beckley,A.J. and Cidlowski,J.A. (2009) Emerging roles of glucocorticoid receptor phosphorylation in modulating glucocorticoid hormone action in health and disease. *IUBMB Life*, **61**, 979–986.
13. Galliher-Beckley,A.J., Williams,J.G. and Cidlowski,J.A. (2011) Ligand-independent prosphorylation of the glucocorticoid receptor integrates cellular signaling stress pathways with nuclear receptor signaling. *Mol. Cell Biol.*, **31**, 4663–4675.
14. Davies,L., Karthikeyan,N., Lynch,J.T., Sial,E.-A., Gkourtsa,A., Demonacos,C. and Krstic-Demonacos,M. (2008) Cross talk of signaling pathways in the regulation of the glucocorticoid receptor function. *Mol. Endocrinol.*, **22**, 1331–1344.
15. Treuter,E. and Venteclef,N. (2011) Transcriptional control of metabolic and inflammatory pathways by nuclear receptor SUMOylation. *Biochim. Biophys. Acta*, **1812**, 909–918.
16. Gill,G. (2004) Sumo and ubiquitin in the nucleus: different functions, similar mechanisms? *Genes Dev.*, **18**, 2046–2059.
17. Tatham,M.H., Jaffray,E., Vaughan,O.A., Desterro,J.M.P., Botting,C.H., Naismith,J.H. and Hay,R.T. (2001) Polymeric chains of SUMO-2 and SUMO-3 are conjucated to protein substrates by SAE1/SAE2 and Ubc9. *J. Biol. Chem.*, **276**, 35368–35374.
18. Kamitani,T., Nguyen,H.P. and Yeh,E.T.H. (1997) Preferential modification of nuclear proteins by a novel ubiquitin-like molecule. *J. Biol. Chem.*, **272**, 14001–14004.
19. Rytinki,M., Kaikkonen,S., Pehkonen,P., Jääskeläinen,T. and Palvimo,J.J. (2009) PIAS proteins: pleiotropic interactors associated with SUMO. *Cell. Mol. Life Sci.*, **66**, 3029–3041.
20. van Wijk,S.J.L. and Timmers,H.T.M. (2010) The family of ubiquitin-conjugating enzymes (E2s): deciding between life and death of proteins. *FASEB J.*, **24**, 981–993.
21. Mukhopadhyay,D. and Dasso,M. (2007) Modification in reverse: the SUMO proteases. *Trends Biochem. Sci.*, **32**, 286–295.

22. Kolli,N., Mikolajczyk,J., Drag,M., Mukhopadhyay,D., Moffatt,N., Dasso,M., Salvesen,G. and Wilkinson,K.D. (2010) Distribution and paralogue specificity of mammalian deSUMOylationg enzymes. *Biochem. J.*, **430**, 335–344.
23. Nacerddine,K., Lehembre,F., Bhaumik,M., Artus,J., Cohen-Tannoudji,M., Babinet,C., Pandolfi,P.P. and Dejean,A. (2005) The SUMO pathway is essential for nuclear integrity and chromosome segregation in mice. *Dev. Cell*, **9**, 769–779.
24. Kaikkonen,S., Jääskeläinen,T., Karvonen,U., Rytinki,M.M., Makkonen,H., Gioeli,D., Paschal,B.M. and Palvimo,J.J. (2009) SUMO-specific protease 1 (SENP1) reverses the hormone-augmented SUMOylation of androgen receptor and modulates gene responses in prostate cancer cells. *Mol. Endocrinol.*, **23**, 292–307.
25. Lin,D.-Y., Huang,Y.-S., Jeng,J.-C., Kuo,H.-Y., Chang,C-C., Chao,T-T., Ho,C-C., Chen,Y.-C., Lin,T.-P., Fang,H.-I. *et al.* (2006) Role of SUMO-interacting motif in Daxx SUMO modification, subnuclear localization, and repression of sumoylated transcription factors. *Mol. Cell*, **24**, 341–354.
26. Ouyang,J. and Gill,G. (2009) SUMO engages multiple corepressors to regulate chromatin structure and transcription. *Epigenetics*, **4**, 440–444.
27. Rytinki,M., Kaikkonen,S., Sutinen,P., Paakinaho,V., Rahkama,V. and Palvimo,J.J. (2012) Dynamic SUMOylation is linked to the activity cycles of androgen receptor in the cell nucleus. *Mol. Cell Biol.*, **32**, 4195–4205.
28. Iñiguez-Lluhí,J.A. and Pearce,D. (2000) A common motif within the negative regulatory regions of multiple factors inhibits their transcriptional synergy. *Mol. Cell. Biol.*, **20**, 6040–6050.
29. Holmstrom,S.R., Chupreta,S., So,A.Y.L. and Iniguez-Lluhi,J.A. (2008) SUMO-mediated inhibition of glucocorticoid receptor synergistic activity depends on stable assembly at the promoter but not on DAXX. *Mol. Endocrinol.*, **22**, 2061–2075.
30. Bladh,L.-G., Liden,J., Pazirandeh,A., Rafter,I., Dahlman-Wright,K., Nilsson,S. and Okret,S. (2005) Identification of target genes involved in the antiproliferative effect of glucocorticoids reveals a role for nuclear factor- κB repression. *Mol. Endocrinol.*, **19**, 632–643.
31. Gentleman,R., Carey,V.J., Bates,D.M., Bolstad,B., Dettling,M., Duboit,S., Ellis,B., Gautier,L., Ge,Y., Gentry,J. *et al.* (2004) Bioconductor: open software development for computational biology and bioinformatics. *Genome Biol.*, **5**, R80.
32. Andrews,S. (2012) FastQC, http://www.bioinformatics.babraham.ac.uk/projects/fastqc/ (23 October 2013, date last accessed).
33. Hannon,G.J. (2012), FASTX-toolkit: FASTQ/A short-reads pre-processing tools. http://hannonlab.cshl.edu/fastx_toolkit/index.html (23 October 2013, date last accessed).
34. Langmead,B., Trapnell,C., Pop,M. and Salzberg,S.L. (2009) Ultrafast and memory-efficient alignment of shorth sequences to the human genome. *Genome Biol.*, **10**, R25.
35. Li,H., Handsaker,B., Wysoker,A., Fennell,T., Ruan,J., Homer,N., Marth,G., Abecasis,G. and Durbin,R. (2009) The sequence alignment/map format and SAMtools. *Bioinformatics*, **25**, 2078–2079.
36. Robinson,J.T., Thorvaldsdottir,H., Winckler,W., Guttman,M., Lander,E.S., Getz,G. and Mesirov,J.P. (2011) Integrative genomics viewer. *Nat. Biotechnol.*, **29**, 24–26.
37. Zhang,Y., Liu,T., Meyer,C.A., Eeckhoute,J., Johnson,D.S., Bernstein,B.E., Nusbaum,C., Myers,R.M., Brown,M., Li,W. *et al.* (2008) Model-based analysis of ChIP-seq (MACS). *Genome Biol.*, **9**, R137.
38. Feng,J., Liu,T., Qin,B., Zhang,Y. and Liu,X.S. (2012) Identifying ChIP-seq enrichment using MACS. *Nat. Protoc.*, **30**, 1728–1740.
39. Landt,S.G., Marinov,G.K., Kundaje,A., Kheradpour,P., Pauli,F., Batzoglou,S., Berstein,B.E., Bickel,P., Brown,J.B., Cayting,P. *et al.* (2012) ChIP-seq guideline and practices of the ENCODE and modENCODE consortia. *Genome Res.*, **22**, 1813–1831.
40. Furey,T.S. (2012) ChIP-seq and beyond: new and improved methodologies to detect and characterize protein-DNA interactions. *Nat. Rev. Genet.*, **13**, 840–852.
41. Liu,T., Ortiz,J.A., Taing,L., Meyer,C.A., Lee,B., Zhang,Y., Shin,H., Wong,S.S., Ma,J., Lei,Y. *et al.* (2011) Cistrome: an integrative platform for transcriptional regulation studies. *Genome Biol.*, **12**, R83.
42. McLean,C.Y., Bristor,D., Hiller,M., Clarke,S.L., Schaar,B.T., Lowe,C.B., Wenger,A.M. and Bejerano,G. (2010) GREAT improves functional interpretation of cis-regulatory regions. *Nat. Biotechnol.*, **28**, 495–501.
43. Alheim,K., Corness,J., Samuelsson,M.K.R., Bladh,L.-G., Murata,T., Nilsson,T. and Okret,S. (2003) Identification of a functional glucocorticoid response element in the promoter of the cyclin-dependent kinase inhibitor p57Kip2. *J. Mol. Endocrinol.*, **30**, 359–368.
44. Blind,R.D. and Garabedian,M.J. (2008) Differential recruitment of glucocorticoid receptor phosphor-isoforms to glucocorticoid-induced genes. *J. Steroid Biochem. Mol. Biol.*, **109**, 150–157.
45. Itani,O.A., Liu,K.Z., Cornish,K.L., Campbell,J.R. and Thomas,C.P. (2002) Glucocorticoids stimulate human sgk1 gene expression by activation of a GRE in its 5′-flanking region. *Am. J. Physiol. Endocrinol. Metab.*, **283**, E971–E979.
46. Frankfurt,O. and Rosen,S.T. (2004) Mechanisms of glucocorticoid-induced apoptosis in hematologic malignancies: updates. *Curr. Opin. Oncol.*, **16**, 553–563.
47. Cubeñas-Potts,C. and Matunis,M.J. (2013) SUMO: a multifaceted modifier of chromatin structure and function. *Dev. Cell*, **24**, 1–12.
48. Flotho,A. and Melchior,F. (2013) Sumoylation: a regulatory protein modification in health and disease. *Annu. Rev. Biochem.*, **82**, 357–385.
49. Samuelsson,M.K.R., Pazirandeh,A., Davani,B. and Okret,S. (1999) p57Kip2, a glucocorticoid-induced inhibitor of cell cycle progression in HeLa cells. *Mol. Endocrinol.*, **13**, 1811–1822.
50. Matsuoka,S., Edwards,M.C., Bai,C., Parker,S., Zhang,P., Baldini,A., Harper,J.W. and Elledge,S.J. (1995) p57KIP2, a structurally distict member of the p21CIP1 Cdk inhibitor family, is a candidate tumor suppressor gene. *Genes Dev.*, **9**, 650–662.
51. Sharrocks,A.D. (2001) The ETS-domain transcription factor family. *Nat. Rev. Mol. Cell Biol.*, **2**, 827–837.
52. Odrowaz,Z. and Sharrocks,A.D. (2012) ELK1 uses different DNA binding modes to regulate functionally distinct classes of target genes. *PLoS Genet.*, **8**, e1002694.
53. Both,J., Wu,T., Bras,J., Schaap,G.R., Bass,F. and Hulsebos,T.J.M. (2012) Identification of novel candidate oncogenes in chromosome region 17p11.2-p12 in human osteosarcome. *PLoS One*, **7**, e30907.
54. Jacquot,J., Tabary,O., Le Rouzic,P. and Clement,A. (2008) Airway epithelial cell inflammatory signaling in cystic fibrosis. *Int. J. Biochem. Cell Biol.*, **40**, 1703–1715.
55. Xu,L.L., Shi,Y., Petrovics,G., Sun,C., Makarem,M., Zhang,W., Sesterhenn,I.A., McLeod,D.G., Sun,L., Moul,J.W. *et al.* (2003) PMEPA1, an androgen-regulated NEDD4-binding protein, exhibits cell growth inhibitory function and decreased expression during prostate cancer progression. *Cancer Res.*, **63**, 4299–4304.
56. Rao,N.A., McCalman,M.T., Moulos,P., Francoijs,K.J., Chatziioannou,A., Kolisis,F.N., Alexis,M.N., Mitsiou,D.J. and Stunnenberg,H.G. (2011) Coactivation of GR and NFKB alters the repertoire of their binding sites and target genes. *Genome Res.*, **21**, 1404–1416.
57. Uhlenhaut,N.H., Barish,G.D., Yu,R.T., Downes,M., Karunasiri,M., Liddle,C., Schwalie,P., Hübner,N. and Evans,R.M. (2012) Insights into negative regulation by the glucocorticoid receptor from genome-wide profiling of inflammatory cistromes. *Mol. Cell*, **49**, 158–171.
58. John,S., Sabo,P.J., Thurman,R.E., Sung,M.H., Biddie,S.C., Johnson,T.A., Hager,G.L. and Stamatoyannopoulos,J.A. (2011) Chromatin accessibility pre-determines glucocorticoid receptor binding patterns. *Nat. Genet.*, **43**, 264–268.
59. Reddy,T.E., Pauli,F., Sprouse,R.O., Neff,N.F., Newberry,K.M., Garabedian,M.J. and Myers,R.M. (2009) Genomic determination of the glucocorticoid response reveals unexpected mechanisms of gene regulation. *Genome Res.*, **19**, 2163–2171.
60. Knutson,T.P., Daniel,A.R., Fan,D., Silverstein,K.A.T., Covington,K.R., Fuqua,S.A.W. and Lange,C.A. (2012) Phosphorylated and sumoylation-deficient progesterone receptors drive proliferative gene signatures during breast cancer progression. *Breast Cancer Res.*, **14**, R95.
61. Bertolotto,C., Lesueur,F., Giuliano,S., Strub,T., de Lichy,M., Bille,K., Dessen,P., d'Hayer,B., Mohamdi,H., Remenieras,A. *et al.* (2011) A SUMOylation-defective MITF germline mutation

predisposes to melanoma and renal carcinoma. *Nature*, **480**, 94–98.
62. Lee,H.Y., Johnson,K.D., Fujiwara,T., Boyer,M.E., Kim,S.I. and Bresnick,E.H. (2009) Controlling hematopoiesis through sumoylation-dependent regulation of a GATA factor. *Mol. Cell*, **36**, 984–995.
63. Lee,F.Y., Faivre,E.J., Suzawa,M., Lontok,E., Ebert,D., Cai,F., Belsham,D.D. and Ingraham,H.A. (2011) Eliminating SF-1 (NR5A1) sumoylation in vivo results in ectopic hedgehog signaling and disruption of endocrine development. *Dev. Cell*, **21**, 315–327.
64. Neyret-Kahn,H., Benhamed,M., Ye,T., LeGras,S., Cossec,J.C., Lapaquette,P., Bischof,O., Ouspenskaia,M., Dasso,M., Seeler,J. *et al*. (2013) Sumoylation at chromatin governs coordinated repression of a transcriptional program essential for cell growth and proliferation. *Genome Res.*, **23**, 1563–1579.
65. Wei,G.-H., Badis,G., Berger,M.F., Kivioja,T., Palin,K., Enge,M., Bonke,M., Jolma,A., Varjosalo,M., Gehrke,A.R. *et al*. (2010) Genome-wide analysis of ETS-family DNA-binding *in vitro* and *in vivo*. *EMBO J.*, **29**, 2147–2160.
66. Molvaersmyr,A.K., Saether,T., Gilfillan,S., Lorenzo,P.I., Kvaløy,H., Matre,V. and Gabrielsen,O.S. (2012) A SUMO-regulated activation function controls synergy of c-Myb through a repressor-activator switch leading to differential p300 recruitment. *Nucleic Acids Res.*, **38**, 4970–4984.